ELSEVIER

European Journal of Pharmacology 393 (2000) 179–195

ejp

www.elsevier.nl/locate/ejphar

α7 Receptor-selective agonists and modes of α7 receptor activation

Roger L. Papke [a,*], Edwin Meyer [a], Tom Nutter [a], Vladimir V. Uteshev [b,1]

[a] *Department of Pharmacology and Therapeutics, Box 100267 JHMHSC, Medical College, University of Florida, Gainesville, FL 32610-0267, USA*
[b] *Department of Molecular Physiology and Biophysics, University of Vermont, Given Building, Burlington, VT 05405, USA*

Accepted 21 January 2000

Abstract

The α7-selective agonists 3-(2,4-dimethoxybenzylidene)-anabaseine (GTS-21), also known as DMXB, and 3-(4-hydroxy,2-methoxybenzylidene)anabaseine (4OH-GTS-21) produce a variety of behavioral and cytoprotective effects that may be related to the activation of either large transient currents at high concentrations or small sustained currents at lower agonist concentrations. We are using acutely dissociated hypothalamic neurons, which express a central nervous system (CNS) α7-type receptor, to test a model for the concentration-dependent desensitization of α7-mediated responses. Our results confirm that 4OH-GTS-21 is a potent activator of neuronal α7 nicotinic-acetylcholine receptor. The rapid application of agonist leads to a brief period of maximal receptor-activation followed by desensitization. Rise rates, decay rates, and the degree to which current was desensitized were all concentration-dependent. Following the initial peak response to a 300-μM 4OH-GTS-21 application, current is reduced to baseline values within about 100 ms. Application of 30 μM 4OH-GTS-21 produced both a transient peak current and a sustained current that decayed only slowly after the removal of agonist. In the case of a 300-μM 4OH-GTS-21 application, after agonist was removed, we saw a rebound response up to the level of the 30-μM sustained current. The data, therefore, suggest that a sufficient level of agonist occupation can be retained on the receptor to promote activation for up to several hundred milliseconds.

Keywords: GTS-21; 4OH-GTS-21; α7 Receptor-selective agonist

1. Introduction

Alzheimer's disease is a progressive neurodegenerative disorder that causes significant memory-related dysfunctions. Therapeutic approaches for this disorder generally fall into either of the two categories: short-term enhancement of memory-function or longer-term protection of vulnerable neuronal populations. Examples of the former class of drug include the cholinesterase inhibitors Tacrine and Aricept, which are clinically accepted. Efforts to develop neuroprotective agents remain largely preclinical in nature and focus on nerve growth factor (NGF) or compounds with NGF-like properties. Recent evidence described below suggests that nicotine receptor agonists may provide both types of therapeutic improvement: behavioral and neuroprotective. The identification of new nicotinic agents with potential therapeutic efficacy has drawn attention to the α7, α-bungarotoxin-sensitive, neuronal nicotinic acetylcholine receptor subtype (De Fiebre et al., 1995). High affinity α-bungarotoxin binding sites in mammalian brain are associated with the α7 nicotinic acetylcholine receptor subunit and are of roughly equal abundance to the high affinity nicotine binding sites which are believed to be primarily composed of α4 and β2 subunits. Despite well-documented effects of nicotine on a wide variety of memory-related behaviors, the effects of this drug in Alzheimer's disease are not clear. In one study, nicotine improved word recall in a manner that approached significance ($P < 0.06$) in Alzheimer's patients at one dose, but the next higher dose caused too many side effects to continue the study (Newhouse et al., 1988). These results suggested that a more selective nicotinic agonist, acting on memory-related pathways without peripheral, and unwanted central nervous system (CNS) actions might elicit more significant memory-related improvement. Along this line, a new experimental agent 3-(2,4-dimethoxybenzylidene)-anabaseine (GTS-21), also known as DMXB,

* Corresponding author. Tel.: +1-352-392-4712; fax: +1-352-392-9696.
E-mail address: rpapke@college.medical.ufl.edu (R.L. Papke).
[1] Present address: Department of Pharmacology and Therapeutics, Box 100267 JHMHSC, University of Florida, Gainesville, FL 32610-0267, USA.

0014-2999/00/$ - see front matter
PII: S0014-2999(00)00009-1

was tested in a small cohort of a Phase I trial and was found to improve memory-related word recall by four separate measures in normal volunteers (Kitagawa et al., 1998).

It has been demonstrated that GTS-21 and its principle-metabolite in primates, 3-(4-hydroxy,2-methoxybenzylidene)anabaseine (4OH-GTS-21), also known as HMBA (Hunter et al., 1994; Martin et al., 1994; Meyer et al., 1994; De Fiebre et al., 1995; Kihara et al., 1997), are selective agonists for the α7-type nicotinic acetylcholine receptor (Meyer et al., 1998a). The use of these selective agonists, as well as the selective antagonists α-bungarotoxin and methylylaconitine (Alkondon et al., 1992; Messi et al., 1997), has done much to increase our understanding about the behavioral and physiological actions of α7 nicotinic acetylcholine receptor. For example, α7 nicotinic acetylcholine receptor has been implicated in the modulation of several memory-related behaviors (Hunter et al., 1994; Martin et al., 1994; Woodruff-Pak et al., 1994; De Fiebre et al., 1995; Meyer et al., 1997, 1998c), hippocampal auditory gating (Stevens et al., 1998), and cell survival (Martin et al., 1994; Kihara et al., 1997; Meyer et al., 1998b,c; Shimohama et al., 1998). With respect to memory-related behaviors, GTS-21 has been found to improve delayed pair-matching behavior in primates (Briggs et al., 1997), eye-blink memory in rabbits (Woodruff-Pak et al., 1994), spatial memory-related behavior in rats (Meyer et al., 1997), and several types of avoidance behaviors in rodents (Arendash et al., 1995; De Fiebre et al., 1995; Meyer et al., 1997). These memory-related actions are consistent with the high concentration of α7 nicotinic acetylcholine receptor and α-bungarotoxin binding sites found in hippocampus, neocortex, and hypothalamus (Clarke et al., 1985; Seguela et al., 1993; Barrantes et al., 1995).

In particular, the histaminergic neurons from the tuberomammillary nucleus of the posterior hypothalamus exhibit high concentrations of α-bungarotoxin binding sites (Clarke et al., 1985). The tuberomammillary nucleus represents the main source of histamine in the CNS and projects axons throughout the brain, including the hippocampal formation (Watanabe et al., 1984; Airaksinen et al., 1991). This nucleus is involved in learning and memory formation and in regulating multiple functions such as sleep and wakefulness, energy and hormonal metabolism, eating, drinking, and sexual behavior (Schwartz et al., 1991; Wada et al., 1991). Lesions of the tuberomammillary nucleus have been found to facilitate learning and memory capacities (Klapdor et al., 1994; Frisch et al., 1998), whereas an electrical stimulation of the tuberomammillary nucleus in freely moving rats has demonstrated inhibitory effects on the efficacy of afferent transmission to the hippocampus during learning-related exploratory behavior (Weiler et al., 1998). Numerous neurofibrillary tangles have been found in the tuberomammillary nucleus of patients with Alzheimer's disease (Saper and German, 1987; Airaksinen et al., 1991; Nakamura et al., 1993). Thus, the tuberomammillary nucleus is implicated not only in normal memory processing, perhaps via regulatory paths to hippocampus, but also in Alzheimer's disease.

Recent electrophysiological studies of acutely dissociated histamine neurons of rats have revealed functional nicotinic responses to fast application of nicotinic, but not muscarinic receptor agonists (Uteshev et al., 1996). The nicotinic responses of the histamine neurons were completely α-bungarotoxin-sensitive, suggesting that these neurons express exclusively α7-type nicotinic acetylcholine receptor. The expression of α7-type nicotinic acetylcholine receptor in histamine neurons of the tuberomammillary nucleus, as well as the involvement of the histamine neurons in the age-related (patho)physiological conditions make these neurons an attractive model for studying the effects of potential therapeutic agents on the physiology and biophysics of α7 nicotinic acetylcholine receptor.

The hypothesis that α7 nicotinic acetylcholine receptor activation might mediate cytoprotective and behavioral effects through the elevation of intracellular calcium is consistent with both the high calcium permeability of this nicotinic acetylcholine receptor (Seguela et al., 1993) and previous reports of α-bungarotoxin-sensitive nicotine-dependent elevations in calcium, coincident with synaptic facilitation (McGehee et al., 1995; Gray et al., 1996). While there is evidence that α7 nicotinic acetylcholine receptor may have a role in synaptic transmission through peripheral ganglia (Zhang et al., 1996), in general, this does not seem to be the case in the CNS. One possible exception was suggested by the work of Frazier et al. (1998) in their study of hippocampal interneurons. However, in order to detect putative α-bungarotoxin-sensitive postsynaptic nicotinic currents, Frazier et al. (1998) required the use of an ''inhibitor cocktail'' designed to suppress currents mediated by NMDA-type glutamate receptors, AMPA-type glutamate receptors, $GABA_A$ receptors, $5\text{-}HT_3$ receptors, and ATP receptors. The inhibitor cocktail also contained 2 μM mecamylamine to ''inhibit non-α7-type nicotinic acetylcholine receptor'', a concentration also reported to be the EC_{50} for the inhibition of α7 nicotinic acetylcholine receptor expressed in *Xenopus* oocytes (Meyer et al., 1998c). In fact, it may be that our understanding of the functional roles played by α7-type nicotinic acetylcholine receptor in the CNS has been impeded by our concept that ligand-gated channels should function like nicotinic acetylcholine receptors of the neuromuscular junction, i.e., they should give large coordinated responses to rapid elevations in neurotransmitter concentration. This concept has, in some sense, been enhanced by the observation that extremely rapid elevations of agonist concentrations have been required to see coordinated activation of α7 nicotinic acetylcholine receptors. Nonetheless, the concept of α7 nicotinic acetylcholine receptors as synaptic receptors is challenged by lack of compelling

evidence for functionally important α-bungarotoxin-sensitive CNS synapses, as well as other observations that suggest unique roles for these nicotinic acetylcholine receptors in neuromodulation (McGehee et al., 1995; Gray et al., 1996) and cytoprotection (Martin et al., 1994; Meyer et al., 1997; Shafron et al., 1997; Shimohama et al., 1998). Also, there is a growing support for the hypothesis that choline may be the endogenous activator of α7 nicotinic acetylcholine receptors. Though not a neurotransmitter, choline is a fully efficacious agonist of α7 nicotinic acetylcholine receptors (Mandelzys et al., 1995; Papke et al., 1996; Albuquerque et al., 1997), and the ubiquitous presence of choline may prevent or perhaps facilitate α7 nicotinic acetylcholine receptor responses to synapse-like acetylcholine release in vivo (Papke et al., 1996).

The nicotinic neuroprotective concept was first established with studies of sympathetic ganglia in the mid-1980s by Koike et al. (1989), based on using choline as the protective agonist during NGF-deprivation. This work was also seminal with respect to demonstrating a role for calcium ions in the nicotinic protection of neurons (Koike et al., 1989). Selective α7-type nicotinic acetylcholine receptor activation has since been shown to exert a neurotrophic function in several neuronal models, including trans-synaptic neocortical neuronal atrophy/loss following nucleus basalis lesions (Sjak-Shie, 1993), brain neuronal cultures treated with NMDA receptor-agonists (Akaike et al., 1994; Shimohama et al., 1998), focal ischemia (Shimohama et al., 1998), axotomized septal neurons in vivo (Martin et al., 1994), differentiated PC12 cells following NGF-deprivation (Martin et al., 1994; Li et al., 1999), and amyloid exposure in various types of cells (Kihara et al., 1997; Meyer et al., 1998a). That GTS-21, 4OH-GTS-21, and related compounds (Meyer et al., 1998a,c) appear to be neuroprotective suggests that α7 receptor activation may slow multiple degenerative processes underlying Alzheimer's disease. It is interesting to note that 4OH-GTS-21, which has considerably greater efficacy at human α7 nicotinic acetylcholine receptor than GTS-21 does, is also considerably more neuroprotective than its parent compound in human-model systems (Meyer et al., 1998a). It appears that GTS-21 may serve as a pro-drug in humans, at least for neuroprotective properties.

An unexpected action of acute exposure to high concentrations of α7 receptor agonists on cultured cells has been neurotoxicity. This toxicity, which is blocked by pretreatment with selective receptor antagonists such as methylylaconitine, was surprising because of the extremely rapid desensitization of α7 nicotinic acetylcholine receptor in the presence of high agonist concentrations. Thus, even a 10-s application of 30 μM GTS-21, followed by receptor-blockade with methylylaconitine, triggered PC12 cell death 24 h later (Li et al., 1999). In contrast, several hours of exposure to lower concentrations of GTS-21 (e.g., 1–10 μM) were necessary for neuroprotection of PC12 cells during NGF-deprivation. These observations clearly suggested that high vs. low levels of α7 receptor activation were acting differently on cell viability through temporally distinct mechanisms. Separate intracellular transduction processes were also implicated, with GTS-21-induced neuroprotection dependent on protein kinase C activation, and neurotoxicity in turn blocked by tyrosine protein kinase inhibitors (Li et al., 1999). Each of these transduction pathways is triggered by calcium ions. Since GTS-21 may increase calcium levels in PC12 cells in a time and concentration-dependent manner, channel properties modulating the influx of this cation may also be involved in the differential actions of these agonists on cell viability.

In this paper, we explore the importance of agonist application kinetics for α7-mediated cytotoxic effects. We also extend our electrophysiological characterization of GTS-21 and 4OH-GTS-21 to the analysis of the receptor-mediated responses of PC12 cells. α7 Receptor-mediated responses are analyzed in terms of peak currents and net charge, indicating that these measures of response differ in their concentration dependence. We describe one possible kinetic model to explain these differences and evaluate some of the predictions from that model with an analysis of α7-type responses in a preparation of acutely dissociated hypothalamic neurons.

2. Methods and materials

2.1. Gel slab drug delivery

A 3% agarose (Schwarz/Mann Biotech, Cleveland, OH) solution in 0.9% saline (pH 7.4 with 5 mM sodium phosphate) was prepared with no drug, 360 μM GTS-21, or 360 μM [^{3}H]hemicholinium-3 (1 Ci/mmol; New England Nuclear, Boston, MA). After heating and cooling, the resulting gels were sliced into slabs containing 120 nmol or GTS-21 or hemicholinium-3, or of equivalent size without drug. These slabs were added to PC12 cell cultures containing 2 ml of Dulbecco's modified Eagle's medium. PC12 cells had been differentiated with 50 nM NGF for 1 week as described previously (Martin et al., 1994). For measurements of drug-release, aliquots of medium were assayed for labeled hemicholinium-3 levels at various times thereafter using liquid scintillation spectrophotometry. The levels of GTS-21 released into the medium were assumed to be the same as those of hemicholinium-3.

For cell viability studies, cells were exposed to 30 μM GTS-21 or agarose slabs (±GTS-21) for 30 min, the time point at which approximately 30 μM GTS-21 was estimated to be the medium concentration in the slab-treated cultures. Medium was replaced at that time in all cultures, and cell density was measured 24 h thereafter, using the NIH imaging program as described previously (Martin et al., 1994).

2.2. Xenopus oocyte expression and recording

Preparation of in vitro synthesized cRNA transcripts and methods of oocyte injection have been described previously (De Fiebre et al., 1995; Papke et al., 1997). Recordings were made 2–7 days following injections. Current responses to drug administration were studied under two electrode voltage clamps at a holding potential of −50 mV. Recordings were made using a Warner Instruments oocyte amplifier interfaced with National Instruments' LabView software. Current electrodes were filled with 250 mM CsCl, 250 mM CsF and 100 mM EGTA, pH 7.3 and had resistances of 0.5–2.0 MΩ. Voltage electrodes were filled with 3 M KCl and had resistances of 1–3 MΩ. Oocytes with resting membrane potentials more positive than −30 mV were not used. Oocytes were placed in a Warner recording chamber with a total volume of 0.6 ml and, unless otherwise noted, were perfused at room temperature with frog Ringer's (115 mM NaCl, 2.5 mM KCl, 10 mM HEPES, pH 7.3, 1.8 mM $CaCl_2$) plus 1 μM atropine to block potential muscarinic receptor responses.

Drugs were diluted in perfusion solution and then applied following pre-loading of 2.0 ml (12-s applications) or 20 ml (120-s application) length of tubing at the terminus of the perfusion system. GTS-21 and 4OH-GTS-21 were supplied by Taiho Pharmaceuticals. Other drugs and chemicals were obtained from Sigma unless otherwise indicated. A Mariotte flask filled with Ringer's was used to maintain a constant hydrostatic pressure for drug deliveries and washes. The rate of drug delivery was 10 ml/min and was consistent for all concentrations and nicotinic acetylcholine receptor subtypes. This represents an agonist application protocol typical for oocyte-expression experiments (Boulter et al., 1987; Luetje and Patrick, 1991; Luetje et al., 1990; Papke and Heinemann, 1991; Papke et al., 1997; Connolly et al., 1992; Seguela et al., 1993).

Responses were normalized for the level of channel expression in each individual cell by measuring the response to an initial application of 300 μM acetylcholine 5 min prior to presentation of the test concentration of acetylcholine. Means and S.E.M. were calculated from the normalized responses of four oocytes for each experimental concentration. α7 Nicotinic acetylcholine receptor responses typically display an increase following the initial application of agonist, which subsequently stabilizes (De Fiebre et al., 1995); therefore, α7-expressing oocytes received two control applications of acetylcholine separated by 5 min at the start of recording, with the second response used for normalization.

An analysis of net charge movement was conducted to determine the effects of low agonist concentrations. For this analysis, we calculated the net charge over either a 1- or 3-min period. The net charge was estimated by summing the current levels measured at 100-ms intervals. The net charge was then normalized to the net charge stimulated by a control acetylcholine application made 5 min before the experimental acetylcholine application.

2.3. Whole-cell patch-clamp recording (PC12 cells)

Three to seven days after plating, PC12 cells attached to tissue culture plastic were perfused (1 ml/min at 22–24°C) with an external recording solution containing 165 mM NaCl, 5 mM KCl, 2 mM $CaCl_2$, 10 mM glucose, 5 mM HEPES, pH = 7.3 (NaOH), with 1 μM atropine. Internal solutions consisted of 70 mM CsCl, 70 mM CsF, 2 mM Mg^{2+}, 10 mM EGTA, 10 mM HEPES, and a high-energy phosphate regenerating cocktail, which was made fresh daily as a stock to give a final concentration in the recording pipette of 20 mM creatine phosphate, 5 mM ATP, and 50 u/ml creatine phosphokinase (Alkondon et al., 1994). Currents were recorded using Sylgard-coated pipettes (1–5 MΩ) and the standard whole-cell patch-clamp configuration. Rapid activation of α7 receptor-mediated currents was achieved using a liquid-filament switch that permits rapid on-rates and sustained concentration changes (Dudel et al., 1990). Signals were recorded using an Axon Instruments Axopatch 200A amplifier, filtered at 10 kHz and digitized at 40 kHz by Digidata interface (Axon) using the program pClamp7.

2.4. Simulations

The model for α7 nicotinic acetylcholine receptor kinetics was developed using SIMU, a program kindly provided by Dr. Tony Auerbach and Fred Sachs (SUNY, Buffalo, NY, www.qub.buffalo.edu). Peak currents were measured by setting 100 channels in the unbound state and then measuring the maximal number of channels simultaneously open over a 100-ms period, following a step to specific agonist concentrations. Four independent replicates were generated for each agonist concentration. In order to calculate steady-state *P*-open values, simulated data were generated for 50 patches containing a single channel. These data were then idealized using SKM, a Vertirbi algorithm-based idealization program (Qin et al., 1996, 1997; Premkumar and Auerbach, 1997), also provided by Drs. Auerbach Qin and Sachs. Values for *P*-open were then calculated for idealized records of 1- or 10-s durations.

2.5. Acute dissociation and electrophysiology of tuberomammillary neurons

Rat brain slices containing histamine neurons have been prepared using a technique described in detail previously (Uteshev et al., 1996). Before each experiment, slices were placed in the recording chamber in the following extracellular solution: 150 mM NaCl, 3 mM KCl, 1.8 mM $CaCl_2$, 1.3 mM $MgCl_2$, 10 mM HEPES, and 10 mM glucose (pH 7.3). Neurons were dissociated manually using two fire-

polished glass needles at the beginning of each experiment. Histamine neurons were distinguished based on their location within the slice as well as on morphological (size and shape) and electrophysiological (profound I_A and I_h currents) properties. All neurons that were identified as histamine neurons demonstrated fast nicotinic responses upon fast applications of nicotinic agonists. Recording patch-clamp pipettes with the resistance of near 1 MΩ were polished and filled with the following intracellular solution: 40 mM CsCl, 100 mM CsF, 30 mM Tris–Cl (pH 7.3). Data were acquired at 5 kHz using pClamp7 software (Axon Instruments).

2.6. Fast agonist application

To deliver nicotinic agonists to the cells, a double-barreled application pipette was built of two fused application tubes (World Precision Instruments, o.d. = 0.35 mm, i.d. = 0.25 mm), firmly mounted on a Burleigh piezoelectric LSS-3200 solution switcher, and its movement was controlled via a computer (pClamp7, Axon Instruments). One tube provided a continuous flow of bath solution and the other could be changed between various experimental agonist solutions. Solutions were then exchanged via the rapid-movement application pipette. Voltage steps used to control the solution switcher were generated by the data acquisition program and conditioned by a filter circuit as previously described (Kabakov and Papke, 1998). Junction potential measurements were used to evaluate solution exchange rates. Specifically, under conditions that precisely mimicked our recording conditions, a recording electrode was placed in the flow of control solution and then a voltage command directed the exchange to a 150-mM CsCl solution. The junction potential measured under such condition scales linearly with the fractional solution exchange (Papke and Thinschmidt, 1998).

3. Results

3.1. Effects of GTS-21 delivery rate on cell survival

We previously showed that the rapid application of 30 μM GTS-21 to PC12 cells could have a cytotoxic effect (Li et al., 1999). We therefore designed an experiment to elucidate how low vs. high agonist concentrations differentially affected α7 receptor homeostasis relative to channel activation and desensitization. Specifically, we investigated whether fast vs. slow increases in agonist concentrations caused similar effects on cell viability, using NGF-differentiated PC12 cells. Our hypothesis was that slow elevations to the same peak concentration would be less toxic than acute agonist-applications because nicotinic acetylcholine receptor would desensitize as the drug-concentrations rose, i.e., before toxic accumulations of calcium ions could occur due to synchronous activation of a sufficiently large number of channels. In order to achieve a slow application of GTS-21, the drug was dissolved in an agarose media, which was allowed to solidify (Papke et al., 1986). The release rate of drug from these slabs was determined in separate experiments using a radio-labeled tracer (Fig. 1A). We determined that 30 min incubation with a drug-loaded gel slab was sufficient to elevate concentrations of the drug in the media to the range of 30–40 μM. While rapid treatment of cells with 30 μM GTS-21 was toxic to the cells, there were no cytotoxic effects when dishes of PC12 cells were exposed to GTS-21-loaded gel slabs for 30 min.

3.2. Nicotinic receptor responses in PC12 cells

We have previously shown that PC12 cells have α-bungarotoxin binding that is displaceable by GTS-21 and 4OH-GTS-21 (Meyer et al., 1998a). In order to confirm that PC12 cells have functional α7-type nicotinic acetylcholine receptor that can be activated by GTS-21 compounds in a manner similar to how they are activated in

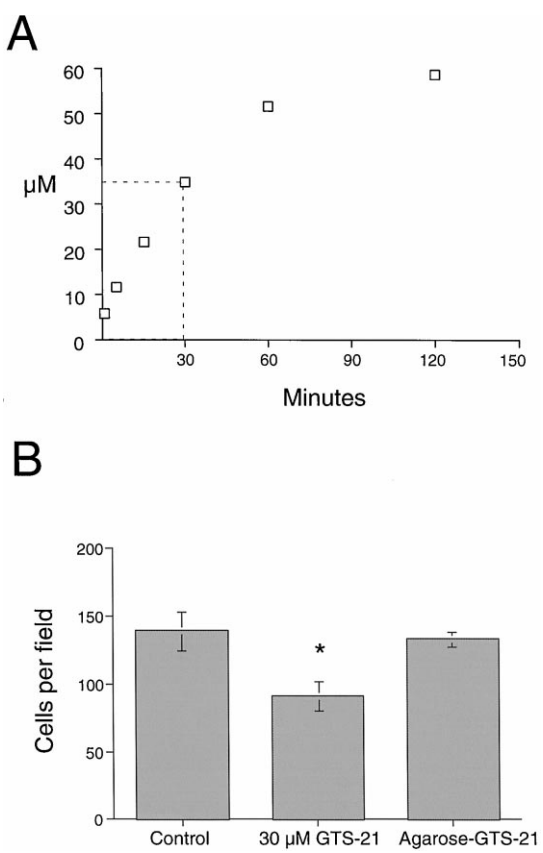

Fig. 1. (A) Release of hemicholinium-3 from agarose gel slabs over time. Slabs containing 120 nmol of [^{3}H]hemicholinium-3 and GTS-21 were placed in 2 ml of medium and aliquots of the medium were assayed for [^{3}H]hemicholinium-3 at the specified intervals. Each value is the mean of duplicate samples. (B) Cell viability 24 h after a 30-min exposure to 30 μM GTS-21, slow-release of GTS-21 to a concentration of 30–40 μM, or agarose-gels containing no GTS-21. Each value is the mean ± S.E.M. of three plates/group; $^*P < 0.05$ compared to no drug treatment control.

oocytes, we conducted an electrophysiological characterization, using a Burleigh fast solution switching device (Kabakov and Papke, 1998). Our results indicated that before differentiation by NGF, only 12% of the PC12 cells tested showed measurable responses to acetylcholine (Fig. 2A, Table 1). However, after cells were differentiated by 10 ng/ml NGF for 1 week, 30% of the cells responded to acetylcholine, with the average responses increasing at least 2-fold (Fig. 2B, Table 1). Responses to acetylcholine in single cells were reproducible, such that when 1 mM acetylcholine was applied to the same cell with a 3-min period between applications, the second responses were equivalent in amplitude to the initial responses. When differentiated PC12 cells were tested for their response to 30 μM GTS-21, 20% showed a response to the initial application (Fig. 2C, Table 1). However, when GTS-21 was reapplied after a 3-min wash, subsequent responses were significantly smaller than the initial responses (Table 1). This is consistent with the residual desensitization or inhibition produced by GTS-21 when it is applied to rat α7 nicotinic acetylcholine receptor expressed in *Xenopus* oocytes. Of the 13 cells tested with an application of 30 μM 4OH-GTS-21, 63% responded (Fig. 2D, Table 1), and in those cells which could be re-tested, the second responses were 100 ± 16% of the size of the initial responses. This is consistent with the low inhibitory activity that this compound has been reported to have for rat α7 nicotinic acetylcholine receptor in *Xenopus* oocytes.

Table 1
Response of differentiated PC12 cells to nicotinic agonists

Agonist	Average initial peak current	Normalized second responses	Percentage responding	*n*
100 μM acetylcholine	200 ± 68 pA	n.a.	21%	24
1 mM acetylcholine	310 ± 87 pA	92 ± 5%	70%	10
30 μM GTS-21	251 ± 67 pA	58 ± 8%	20%	82
30 μM 4OH-GTS-21	86 ± 27 pA	100 ± 16%	63%	13

3.3. Evaluation of α7-acetylcholine receptor-mediated responses through measurements of net charge

The low peak currents of α7 nicotinic acetylcholine receptors in response to acetylcholine applications in the range of 10–30 μM do not show the profound desensitization associated with the presence of only slightly higher acetylcholine concentrations (Papke and Thinschmidt, 1998). This implies that the most effective activation of these channels for the regulation of intracellular calcium in the long-term presence of agonists may be obtained with relatively low agonist concentrations. We can illustrate this trend just through a comparison of peak responses to net charge in the responses we normally study. One such experiment is illustrated in Fig. 3. Note: these experiments were conducted in Ringer's solution in which barium was substituted for calcium (barium-Ringer's) in order to decrease the contribution of the late onset calcium-dependent chloride currents to our measurements. In these experiments, the peak responses to the brief (12 s) pulses of 30 μM acetylcholine were only 37 ± 8% of the 300 μM acetylcholine controls. However, the net charge that was stimulated by 30 μM acetylcholine was 70 ± 6% of the net charge transferred by a 300-μM acetylcholine application (Fig. 3B). In such an experiment, the net charge transfer function is only transiently greater during the initial phase of a high agonist concentration application,

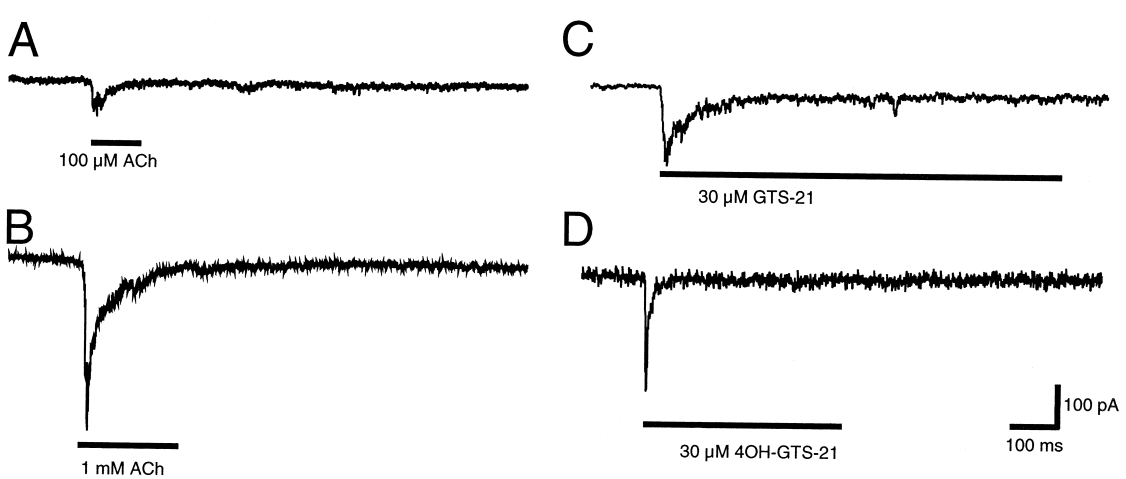

Fig. 2. Response of PC12 cells to the application of nicotinic agonists. (A) Representative response of an undifferentiated PC12 cell to 100 μM ACh application. Of 17 cells tested which had typical undifferentiated morphology, 12% responded to ACh application with an average response to 100 μM ACh of 85 ± 5 pA. (B) Representative response of a differentiated PC12 cell to 1 mM ACh application. (C) Representative response of a differentiated PC12 cell to the application of 30 μM GTS-21. (D) Representative response of a differentiated PC12 cell to the application of 30 μM 4OH-GTS-21. See Table 1 for summary of results obtained with differentiated PC12 cells.

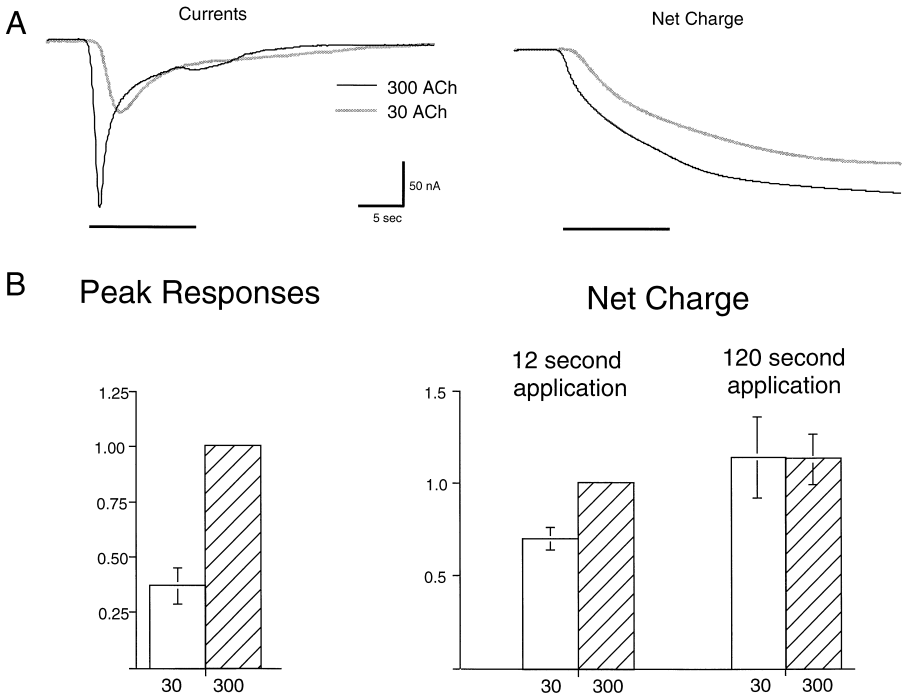

Fig. 3. (A) Peak currents (left) and net charge (right) made from a human α7 expressing oocyte, in response to 12-s applications of either 300 μM acetylcholine (thin black line) or 30 μM acetylcholine (thick gray line). In order to diminish the contributions of calcium-dependent chloride currents to late phase current, these measurements were made in Ringer's solution in which barium was substituted for calcium. (B) The average peak and net charge values to the application 30 and 300 μM acetylcholine. Data for peak responses obtained when the agonist application was 12 s in duration are presented on the left. Data on the right compare normal 12 applications with net charge measurements made when acetylcholine applications were extended to 120 s in duration.

before the full concentration is achieved in the chamber. In the later stages of the response, charge flow is actually greater in the low agonist condition.

These results suggested that in the continued presence of agonist, charge associated with a relatively low agonist application would continue to accumulate, while that activated by the higher concentration would not. To test this, 2-min applications were made of agonist solutions in barium-Ringer's. The net charge integrated over a 3-min period was the same for a response stimulated by 30 μM acetylcholine as that for a response activated by 300 μM acetylcholine. Specifically, the 2-min application of 30 μM acetylcholine stimulated 114 ± 22% as much current as a 12-s application of 300 μM acetylcholine. A 2-min application of 300 μM acetylcholine stimulated only 113 ± 14% as much current as a 12-s application of the same solution (Fig. 3).

3.4. A hypothetical kinetic scheme for α7 nicotinic acetylcholine receptor activation

Concentration–response functions for human α7 nicotinic acetylcholine receptor have been reported for this receptor subtype expressed in oocytes and in human embryonic kidney (HEK) cells (Gopalakrishnan et al., 1995). In spite of a 30-fold difference in time scale, the HEK responses bear a striking resemblance to the data obtained in *Xenopus* oocytes (Papke and Thinschmidt, 1998). This might be taken to suggest that the process which limits the kinetics for desensitization is not strictly time-dependent, but rather a specifically concentration-dependent process. In other words, transition into desensitized states may not be solely described by first-order processes that follow from peri-activational states (i.e., liganded closed states competent for opening as first-order processes), as in traditional models. Specifically, what is perceived as a desensitization process that limits the α7 nicotinic acetylcholine receptor response to the application of high agonist concentration may be driven by a pseudo-first-order process, one that is associated with agonist binding per se. Such a process of pseudo-first-order desensitization would generate maximal concentration-dependent responses that would be independent of the rate at which the optimal concentration is obtained. For example, if peak responses to an instantaneous concentration change are maximal at 200 μM, and higher concentrations lead to smaller responses, then either the fast application of 1 mM or the slow application of 1 mM would lead to their respective maximal responses when the instantaneous concentration was not more than 200 μM. This possibility has been supported by our concentration correction studies conducted using *Xenopus* oocytes. We showed that when high agonist concentrations were applied to α7-expressing cells,

peak currents were obtained long before complete solution exchange could occur (Papke and Thinschmidt, 1998).

A traditional model for desensitization such as that proposed by Katz and Thesleff (1957) predicts increased decay rates at high agonist concentrations, but also predicts progressive increases in peak response amplitude throughout the concentration range (data not shown). The Katz and Thesleff model has been shown to provide a reasonable description of many nicotinic acetylcholine receptor subtypes (Marks et al., 1994). However, in some cases, there was an apparent decrease in peak responses at high agonist concentrations, which could be explained by concentration-dependent channel block by agonist (Sine and Steinbach, 1986; Papke et al., 1988). While it cannot be excluded that the rapid desensitization of α7-type nicotinic acetylcholine receptor may involve some sort of channel block by agonist, the apparent lack of voltage dependence in α7 fast desensitization (Uteshev et al., 1996) would argue against this. Therefore, we sought to develop a kinetic model that might provide a novel perspective on the possible mechanism that could underlie α7 rapid desensitization.

Since α7 nicotinic acetylcholine receptor subunits form functional homomeric receptors with the potential for up to five identical agonist binding sites, we investigated models that were based on the assumption that the α7 nicotinic acetylcholine receptor was effectively opened by the binding of two agonist molecules, a level of agonist occupancy comparable to that required to activate muscle type nicotinic acetylcholine receptor or other neuronal nicotinic acetylcholine receptor, but that further agonist binding events led to additional closed conformations. The most basic forms of such a model predicted concentration-dependent decreases in peak currents, but also predicted maximal steady-state currents of about 30–40% maximum *P*-open, which were too large to be consistent with the experimental data (data not shown).

Therefore, a class of slow desensitized states was added to the model (see Fig. 4). With this fractional occupation–activation model, the maximal steady-state *P*-open approaches that observed experimentally (i.e., approximately 4–8% of the maximal peak current (Papke and Thinschmidt, 1998)). At high agonist concentrations, the desensitizing state is intrinsically absorbing, such that transitions out of this state are slow, as long as agonist is bound. However, experimental data indicate that recovery from desensitization is relatively rapid once the agonist is removed from the chamber. Therefore, in this fractional occupation–activation model, we assume that transitions out of the desensitized state are progressively faster with lower levels of agonist occupancy, reflected in the scaling factors for d^+. Note that although six levels of agonist binding (0–5) are included, this model actually requires no more parameters than the most basic model for desensitization (Katz and Thesleff, 1957), since binding to each subunit is assumed to be independent. Simulations of 100 channels following the behavior described in the fractional occupation–activation model (Fig. 4) predict the currents in Fig. 4B, which resemble those recorded from oocytes (Papke and Thinschmidt, 1998) and HEK cells (Gopalakrishnan et al., 1995). Note that the initial parameters of the model were chosen to reproduce the EC_{50} of an experimental instantaneous concentration curve, and so the concentrations in the simulation roughly correspond to the values for concentration-corrected oocyte responses (Papke and Thinschmidt, 1998).

Fig. 4B illustrates a complete set of representative traces for a simulation of one hundred 1-pA channels following the fractional occupation–activation model (Fig. 4). Unlike the experimental results, which require a finite time for solution exchange, these simulations represent the behavior of channels after a theoretically instantaneous jump to the indicated concentration. Up to the concentration of 200 μM, the responses have progressively increased peak amplitudes and show acceleration in the time to peak. At concentrations above 300 μM, these effects reverse, suggesting that if concentration were ramped from 0 to 1 mM, the maximal response would be observed at the time before the concentration reached 200 μM. With further increase in concentration, the response would be diminished by both time-dependent and concentration-dependent processes.

Fig. 4. (A) A fractional occupation–activation scheme for α7 nicotinic acetylcholine receptor (see text). (B) Representative traces of the simulated responses of 100 channels with activation kinetics described by the model in panel A. When open, each channel will contribute 1 pA of current. Each trace represents 20 ms of simulation, beginning with theoretically instantaneous increases in agonist concentration at the points indicated by the arrows. Shown in the left hand panel are the responses associated with increasing the agonist concentration from 1 to 200 μM. In the right hand panel are the responses associated with increasing the agonist concentration above 200 μM. Note that peak currents decrease when agonist concentration is increased in this range. (C) Representative simulations of steady-state currents for 20 and 200 μM acetylcholine. The traces represent the final 50 ms of 10-s simulations for 100 channels, each of which contributing 1 pA of current when open. The dashed lines represent the zero current levels. For each of these concentrations, steady state is achieved after less than 1 s (see Table 2). (D) The concentration–response relationships predicted by the model in the fractional occupation–activation model (Fig. 4) for steady-state currents (squares) and peak currents (circles). The left-hand axis indicates the *P*-open values relative to the maximum obtainable for the two conditions. On the right are axes that indicate the actual *P*-open values for the two measures. Both measurements show an increase over a certain concentration range (filled symbols) then decrease at higher concentrations (open circles). See Table 3 for the fit parameters.

The responses generated by our simulation can be characterized in terms of both the peak and steady-state components. Experimental α7 responses in other systems (Alkondon and Albuquerque, 1993; Zhang et al., 1994), as well as from oocytes, suggest that low levels of tonic activity can be supported by prolonged application of relatively low concentrations of agonist. Consistent with these observations, the fractional occupation–activation model (Fig. 4) predicts roughly twice as much steady-state current after the model has been allowed to equilibrate for

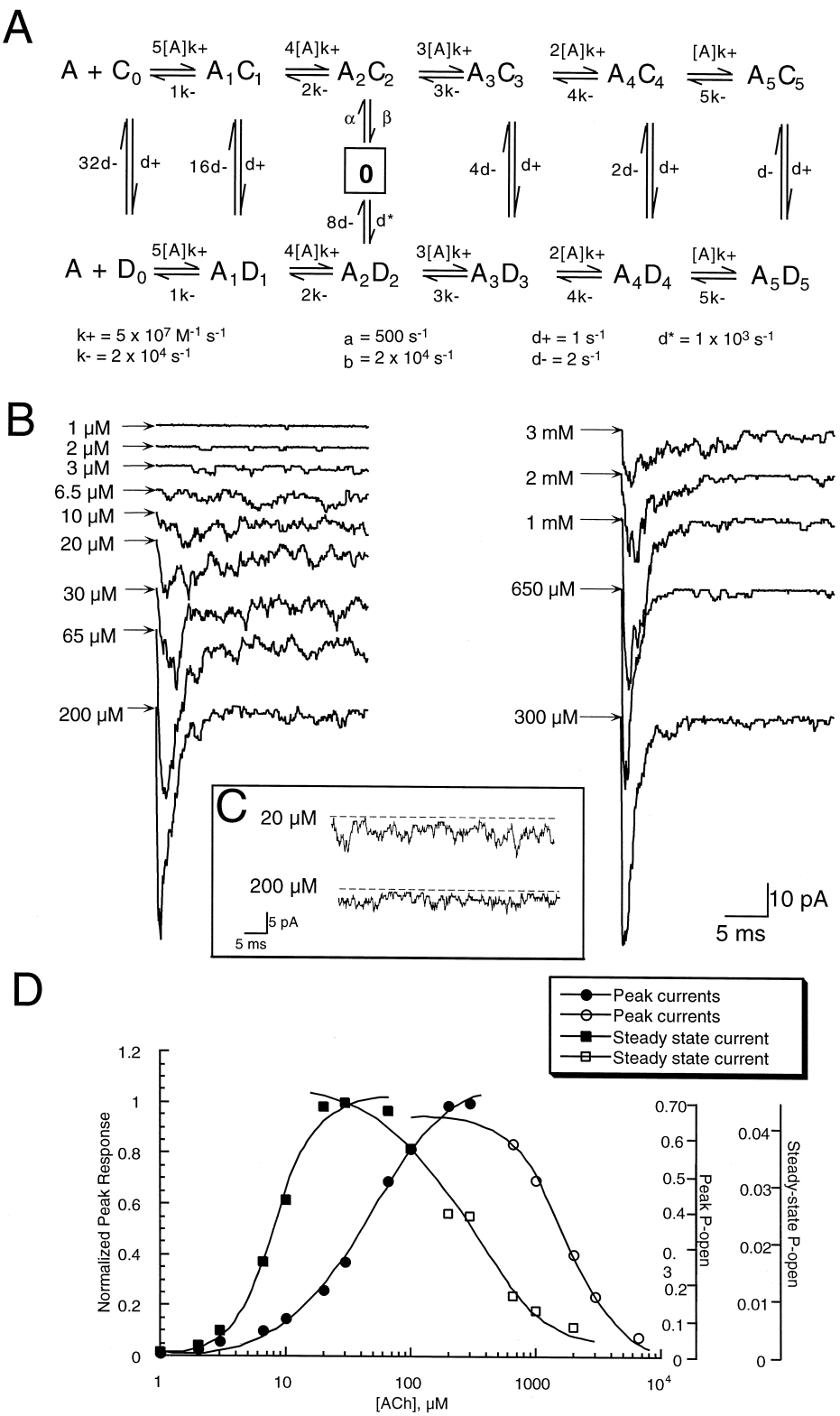

10 s at 20 μM acetylcholine than would be predicted after a similar equilibration time in 200 μM acetylcholine (Fig. 4C).

In Fig. 4D, we show the concentration–response relationships for both peak currents and steady-state *P*-open (measured for a 1-s concentration jump). Each relationship is fit by two functions, one for increases in the low concentration range and another for decreases in the high concentration range (parameters of the curve fits are given in Table 2). With the rate constants given, the model predicts a maximum *P*-open at the peak of a 200-μM response, corresponding to 70% of the channels open simultaneously for a brief period of time. The steady-state *P*-open function is maximal at 20 μM and at that concentration, there is an average of 4% of the channels open at any time. As shown in Table 3, at concentrations of 200 μM acetylcholine, steady-state *P*-open predicted by the model is essentially equilibrated after 1 s, compared to a 10-s value. However, the average *P*-open calculated for a 10-s period after the jump to 2 mM acetylcholine was significantly less than the average *P*-open for the first 1 s at 2 mM, due to a shift in the weighting of the average between the brief initial period of relatively high *P*-open and the ultimately low steady-state *P*-open.

3.5. α7-Bungarotoxin-sensitive responses of acutely dissociated hypothalamic neurons

Neurons were acutely dissociated from fresh slices of rat hypothalamus, and histamine neurons of the tuberomammillary nucleus were identified based on morphological criteria, as previously described (Uteshev et al., 1996). All tuberomammillary neurons tested ($n > 25$) showed robust responses to the application of nicotinic agonists (acetylcholine or 4OH-GTS-21) with the rapid desensitization that is characteristic of α7-type nicotinic acetylcholine receptor. Shown in Fig. 5A are representative responses to the application of either 1 mM acetylcholine or 100 μM 4OH-GTS-21, obtained from the same tuberomammillary neuron. Responses to acetylcholine and 4OH-GTS-21 were completely sensitive to block by α-bungarotoxin.

Under our experimental conditions, the nicotinic responses of tuberomammillary neurons remained of stable amplitude for long periods of time. A sequence of six responses to 200-ms applications of 300 μM 4OH-GTS-21, obtained at 30-s intervals, are shown in Fig. 6A. Therefore, although there was a profound rapid desensitization during each 200-ms application, receptors were fully recovered to the same activatable status after only 30 s.

It has been previously reported (Uteshev et al., 1996), that in the absence of extracellular magnesium, tuberomammillary neurons show a degree of inward rectification of their current–voltage relationships similar to what has been reported for the α7-type (type 1A) responses recorded in cultured hippocampal neurons under similar conditions (Alkondon et al., 1994). However, when 2 mM $MgCl_2$ was added to the bath, the outward currents of cultured hippocampal neurons were suppressed (Alkondon et al., 1994). The present study was conducted with 1.3 mM $MgCl_2$ in the bath, and we frequently had difficulties maintaining stabile recordings at positive holding potentials, and thus at measuring outward currents. However, in neurons which could be studied at positive potentials, we observed inward rectification of their current–voltage relationship (Fig. 6B) similar to what was previously reported for tuberomammillary neurons when recorded in the absence of extracellular magnesium (Uteshev et al., 1996).

Table 2
Curve fits of simulated data *P*-open concentration–response curves

	Steady-state *P*-open		Peak *P*-open	
	EC_{50}	*n*	EC_{50}	*n*
Activation[a]	8 ± 0.4 μM	2.6 ± 0.35	47 ± 4 μM	1.30 ± 0.08
Inhibition[b]	273 ± 37 μM	−1.24 ± 0.16	1751 ± 211 μM	−2.06 ± 0.45

[a]Activation refers to the concentration range in which *P*-open increases with increasing concentration.

[b]Inhibition refers to the concentration range in which responses were observed to decrease at higher agonist concentration.

Table 3
Average *P*-open of simulated data

[Acetylcholine]	1 s Concentration jump	10 s Concentration jump
2 μM	0.0020 ± 0.0010[a]	0.0023 ± 0.0002
20 μM	0.0438 ± 0.0026	0.0412 ± 0.0010
200 μM	0.0251 ± 0.0019	0.0252 ± 0.0007
2 mM	0.0054 ± 0.0016	0.0032 ± 0.0002

[a]S.E.M. based on nine independent simulations.

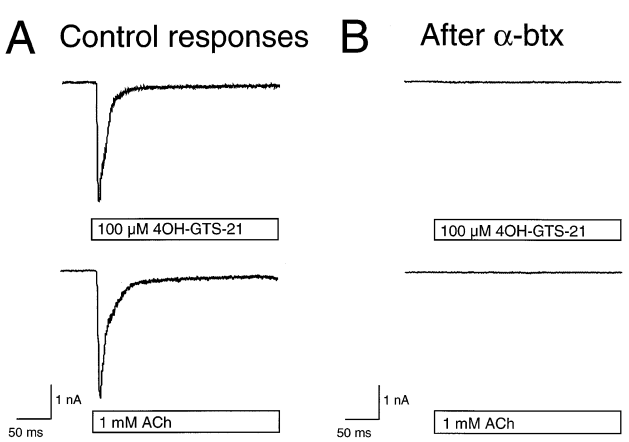

Fig. 5. Agonist selectivity of tuberomammillary neurons. (A) Examples of responses to 1 mM of acetylcholine and 100 μM of 4OH-GTS-21 recorded from the same neuron are shown. The result suggests 10-fold higher potency of 4OH-GTS-21 compared to acetylcholine on tuberomammillary neuronal α7 nicotinic acetylcholine receptor. (B) The responses to 100 μM of 4OH-GTS-21 and 1 mM acetylcholine were blocked completely by an 8-min exposure to 1.5 μM of α-bungarotoxin, an α7 nicotinic receptor selective antagonist (same neuron as in A). The timing of agonist applications is marked by the bars. Holding potential was −80 mV.

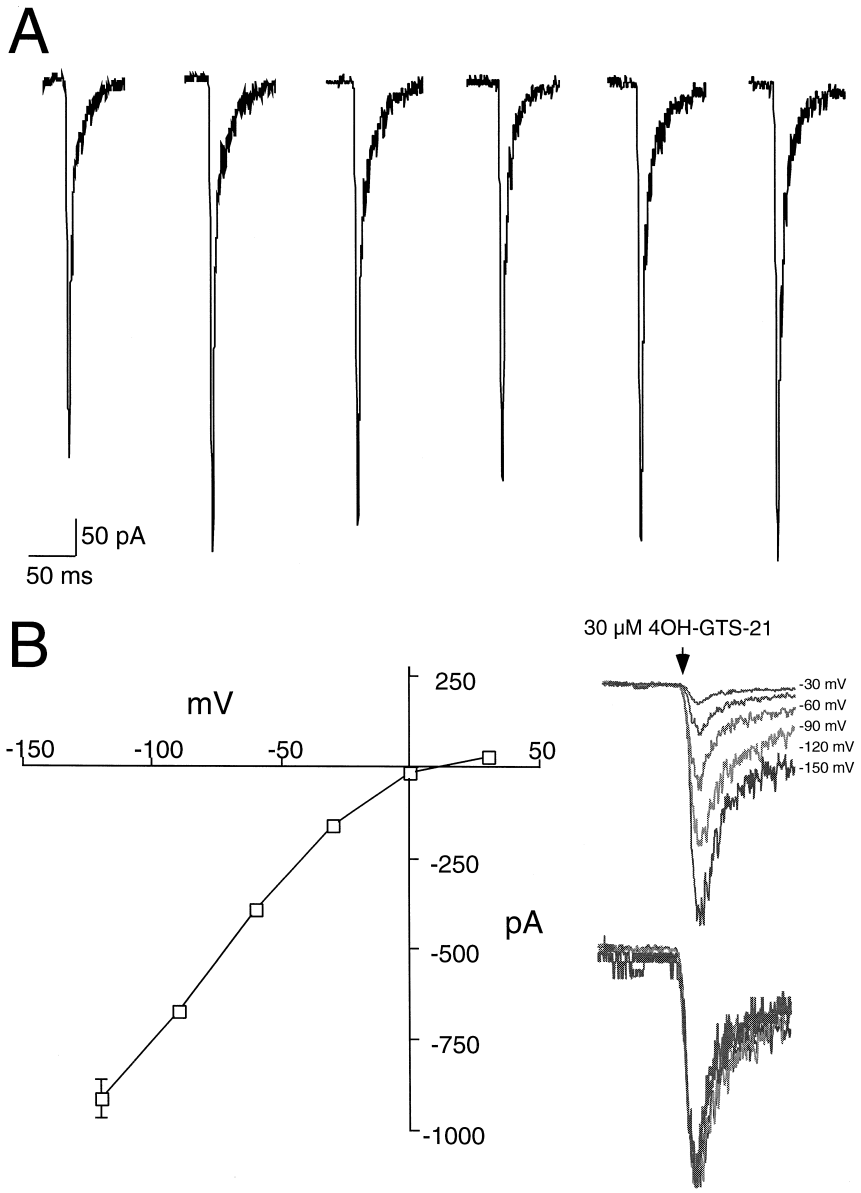

Fig. 6. (A) Stability of the nicotinic responses. Six typical responses of a histamine neuron to repeated applications of 300 μM of 4OH-GTS-21 are shown. The neuron was held at −90 mV and the agonist was applied every 30 s. Between the applications, the neuron was held in a stream of the external solution. (B) A current vs. voltage relationship for whole-cell responses to the application of 300 μM 4OH-GTS-21 is shown. Each point on the graph represents an average of at least three responses obtained from a single histamine neuron. The relationship shows a significant inward rectification near the reversal potential and at positive potentials. The right portion of the figure shows examples of the nicotinic responses of the same cell to the application of 30 μM 4OH-GTS-21, obtained at different voltages as indicated (upper figure), and the same responses when scaled to the same peak amplitude (lower figure). As seen from the excellent alignment of the scaled currents, voltages in the range between −150 and −30 mV do not seem to influence the desensitization onset.

The response kinetics of tuberomammillary neurons to the application of 4OH-GTS-21 showed a strong concentration dependence. The response to the application of 30 μM 4OH-GTS-21 had a lower peak and was slower to reach that peak value compared to the response to the application of 300 μM 4OH-GTS-21 (Fig. 7A). Although the peak responses to 30 4OH-GTS-21 were smaller than the peak responses to 300 μM 4OH-GTS-21, the net charge integrated over the 200-ms application period was much greater for current evoked by the lower agonist concentration ($P < 0.01$). This was apparently due to the concentration dependence of rapid desensitization. The average net charge of a representative single cell evoked by 300 μM 4OH-GTS-21 was 8177 ± 1462 pA ms. In the same cell, the average net charge evoked by 30 μM 4OH-GTS-21 was about three times larger (24232 ± 2972 pA ms).

Using our standard experimental conditions, solution exchange is accomplished with a time constant of about 4 ms (Fig. 7B), as measured by CsCl junction potentials. The

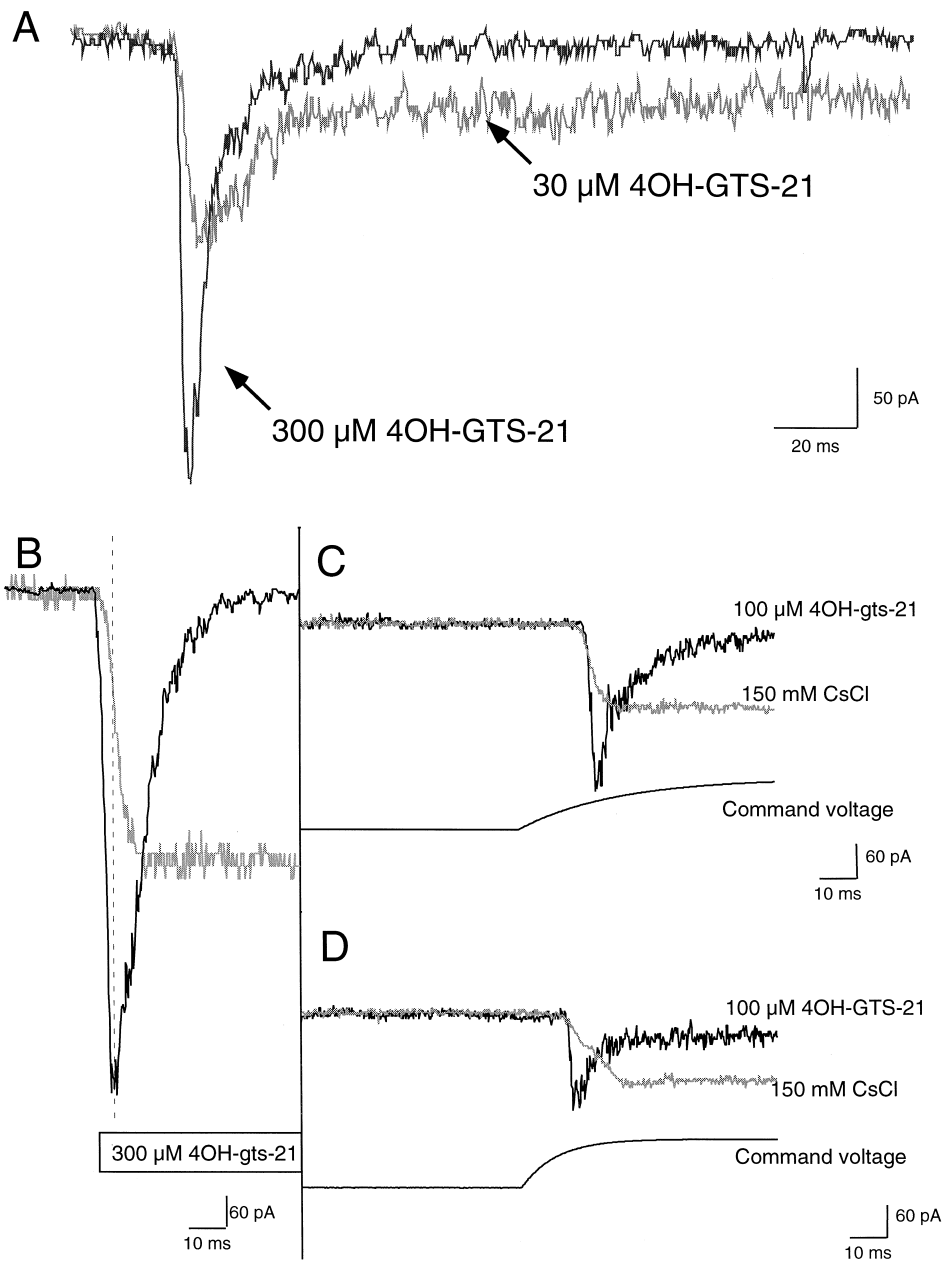

Fig. 7. Concentration dependence of the nicotinic responses to 4OH-GTS-21. (A) Two responses to applications of high and low concentrations of 4OH-GTS-21 to the same histamine neuron are presented. Holding potential was −90 mV. Note a difference in the peak amplitude vs. equilibrium current amplitude depending on the agonist concentration used. (B) Current response kinetics (black line) compared to speed of solution exchange measured by CsCl junction potential (gray line). The dashed line indicates the alignment of the peak response with the rising phase of the solution exchange. (C) Response of the same histamine neuron shown in (D) to application of 100 μM of 4OH-GTS-21, recorded with a different application speed (see text). Holding potential was −80 mV.

peak responses of tuberomammillary neurons to the application of high agonist concentrations occur well before the solution exchange could have been complete (Fig. 7B). This is similar to what has been observed in the oocyte system, even though the absolute agonist application rates differed by several orders of magnitude between these two systems. Note that the piezo-electric solution switcher responds poorly to an extremely fast change in command voltage (e.g., a voltage step command) and so requires signal conditioning to produce smooth and rapid movement of the application pipette (Kabakov and Papke, 1998). As a further demonstration of the sensitivity of peak responses to the timing of agonist exchange, we changed agonist application rates by adjusting the time constant of our voltage command signal. Normally, we use a command voltage that has been conditioned with a resistance–capacitance (RC) filter that has a time constant of 33 ms (Fig. 7C); this produces a solution exchange with a time

constant of 4 ms. As shown in Fig. 7D, reducing the RC time constant of the filter to 7 ms produces movement of the application pipette sooner, but the movement itself is slower, so that the time constant of solution exchange is 13 ms. This slowing of the application rate delayed the peak response to 100 μM 4OH-GST-21 and reduced the peak amplitude.

Our agonist application method allows for a rapid, complete and reversible agonist application. As shown in Fig. 7, during an agonist application, 300 μM 4OH-GTS-21 produces complete desensitization, while 30 μM 4OH-GTS-21 supports some sustained, essentially steady-state current. Interestingly, after the end of the 200-ms agonist application, the apparent steady-state current of the 30

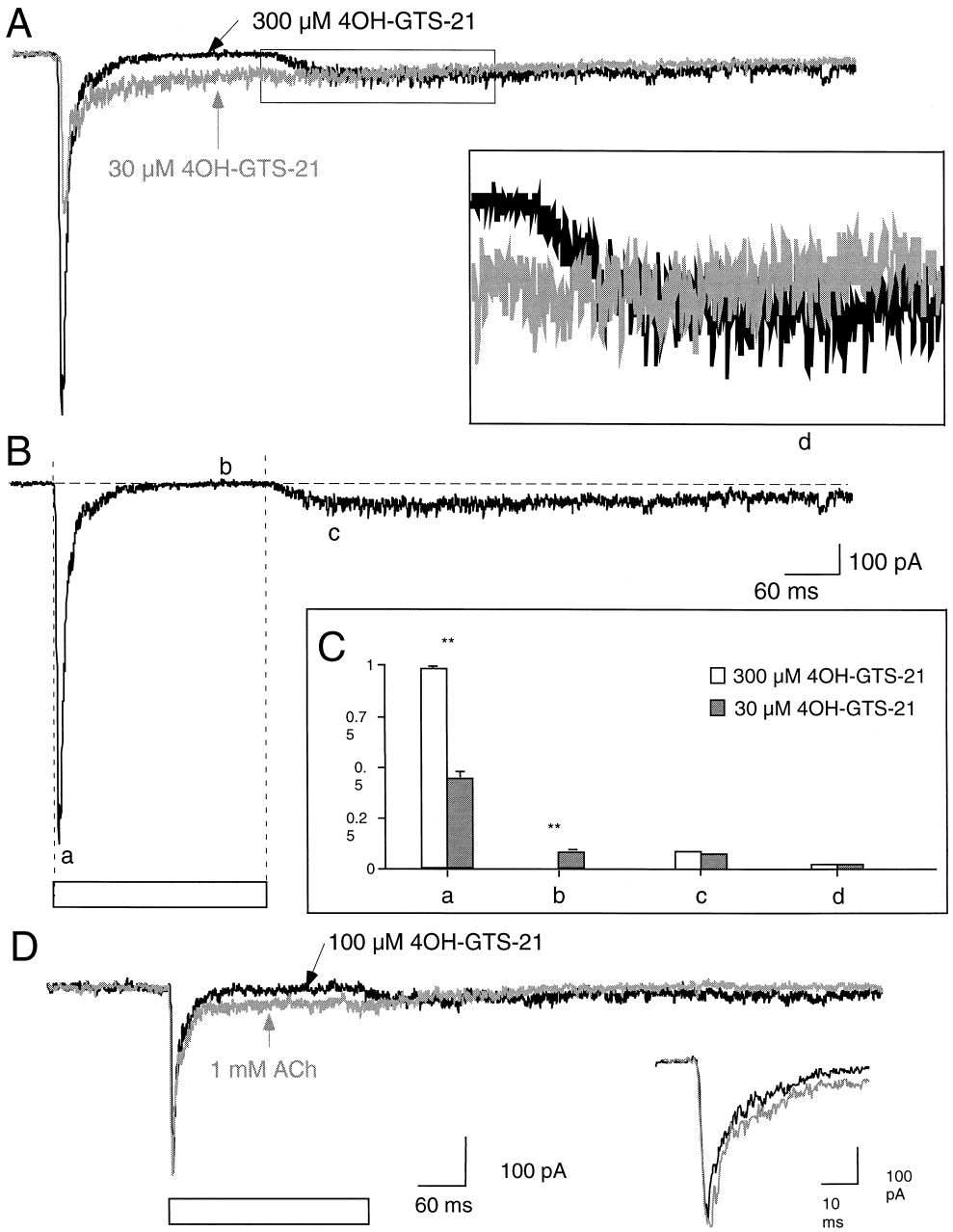

Fig. 8. Concentration dependence and agonist dependence of rebound currents. (A) Responses to high and low concentrations of 4OH-GTS-21 are shown. The slow desensitization tail of the response to 30 μM agonist concentration equilibrates to the same level as the rebound response to 300 μM concentration of 4OH-GTS-21 recorded from the same neuron. The insert shows the desensitization tails of both responses at the time of the rebound. Holding potential was −90 mV. (B–C) Amplitudes of responses to high and low agonist concentrations were compared at different times after the agonist application. (B) A schematic representation of the timing where the amplitude measurements have been taken. (C) A graphic presentation of the analysis of responses obtained from five histamine neurons. (D) Comparison of responses evoked by application of 100 μM 4OH-GTS-21 and 1 mM acetylcholine on the same histamine neuron (same responses shown in Fig. 5). Note the differences in the rebound: a rebound was evoked by the removal of 100 μM 4OH-GTS-21, demonstrating that this agonist was more effective at promoting a reversible form of desensitization (or inhibition), compared to acetylcholine applied at a concentration (1 mM) that evoked a peak response of a similar amplitude.

μM-evoked response decays only slowly, suggesting that agonist may remain bound to the receptor and support further transitions into the open state (Fig. 8A). In the case of a 300-μM OH-GTS-21 application, we see that there is actually a rebound in current at the end of the agonist application that rises to a level that is equivalent to the equilibrium activation of a cell exposed to 30 μM 4OH-GTS-21 (Fig. 8A). We evaluated the responses of five tuberomammillary neurons to applications of both 30 μM 4OH-GTS-21 and 300 μM 4OH-GTS-21 (three responses to each concentration in each neuron) and measured the response amplitudes at different time points indicated in Fig. 8C. We measured the peaks (a), the current just before the end of the agonist application (b), current 50 ms after the agonist application was finished (c), corresponding to the peak of the rebound current, and the average current during the last 100 ms of the 1-s sweeps of acquired data (see Fig. 8B). As shown in Fig. 8C, the peak responses to 30 μM 4OH-GTS-21 were only 45% of the amplitude of the 300-μM 4OH-GTS-21 responses. However, by the end of the application, 300-μM 4OH-GTS-21 responses had declined to zero (0.002 ± 0.003 times the peak amplitude), while the 30-μM 4OH-GTS-21 responses remained at $8 \pm 2\%$ of the amplitude of the 300-μM 4OH-GTS-21 peaks. The rebound of the 300-μM 4OH-GTS-21 responses restored both to the same level, and both responses decayed slowly over the next several hundred milliseconds. As noted above (Fig. 6), a 30-s wash was sufficient to return the α7-type nicotinic acetylcholine receptor of the tuberomammillary neurons to a fully activatable state.

Comparison of 1 mM acetylcholine-evoked responses to 100-μM 4OH-GTS-21 responses supports the concept that acetylcholine behaves as a less potent agonist, producing currents that are slower to reach maximum and showing significant amounts of sustained current (Fig. 8D). However, since application kinetics are probably limiting for both the acetylcholine and the 4OH-GTS-21 responses, both of these drugs will need to be tested through a larger concentration range to determine their relative efficacies for both peak and equilibrium currents. Nonetheless, as can be seen from Fig. 8D, complete equilibrium current suppression and a slow rebound occurs with 100 μM 4OH-GTS-21, while the responses to 1 mM acetylcholine are more like the 30-μM 4OH-GTS-21 responses, in that they show only a partial decay to what might approach a steady-state level.

4. Discussion

A great deal of useful information about α7 nicotinic acetylcholine receptor has come from the study of the cloned receptors in various expression systems. We previously demonstrated that the anabaseine derivatives GTS-21 and 4OH-GTS-21 were selective activators of α7 nicotinic acetylcholine receptor expressed in *Xenopus* oocytes. In the present study, we show that these drugs will also activate the receptors in PC12 cells and acutely dissociated brain neurons. In the case of PC12 cells, we also show that, as described in the oocyte system, GTS-21 application can produce a residual inhibition of subsequent responses, while 4OH-GTS-21 does not have this effect.

Choline is a fully efficacious agonist of α7 nicotinic acetylcholine receptors (Mandelzys et al., 1995; Papke et al., 1996), and drugs like GTS-21 may selectively target the α7 receptor subtype (De Fiebre et al., 1995), much like choline does. Therefore, these drugs could work through low concentration effects, which may produce significant steady-state α7 activation. Indeed, the functional efficacy of α7-selective agents may depend on these limiting low concentration effects. Moreover, a certain amount of therapeutic safety may exist for α7 agonists, due to the concentration-dependent limitation to the amount of receptor-mediated calcium flux, which would prevent the sort of direct excitotoxicity associated with excessive activation of the NMDA-type glutamate receptors. Our gel slab experiments support the idea that, due to the unique desensitization of α7 nicotinic acetylcholine receptor, the slow delivery of agonists, as in a therapeutic context, would lessen any possible toxic effects of over-activation of these calcium-permeable receptors.

This observation leads to the concept that in vivo, the α7 nicotinic acetylcholine receptor of the brain may best be thought of as tonic rather than phasic receptors. In order to put this concept into a meaningful context, we have conducted analysis of α7 receptor responses in terms of both peak currents and net charge. This analysis suggests that these functions have very different dose dependencies and leads us to attempt to devise a model that could account for these functional modalities.

The fractional occupation–activation model (Fig. 4) illustrates one way in which apparent desensitization might become a time-independent function of agonist concentration. Such a model can explain how concentration ramps (associated with finite solution exchange rates) on different time scales would activate maximal responses at specific points in the solution exchange process that would be determined by the specific (time-independent) concentration change rather than elapsed time. The model is based on independent binding sites, equal to the number of identical subunits that may be present in the receptor subunit complex, and then assumes that gating of an α7 nicotinic acetylcholine receptor would require only the same degree of agonist occupancy that has been shown to be required by other nicotinic acetylcholine receptor subtypes (i.e., two agonist molecules bound per open receptor (Sine and Taylor, 1980)). The essential feature of the model that creates a direct concentration dependence for desensitization is the concept that levels of agonist occupancy greater than two per complex would lead to further conformational change and result in agonist-bound, but non-conducting states. That is, two twists of the transmem-

brane helices may open the ion pore, but further twists, associated with higher levels of agonist occupancy, close it again. Note the model is relatively parsimonious in that it requires no more rate constants than a minimal model for desensitization (Katz and Thesleff, 1957), since all five subunits are assumed to be identical and independent. While this model can be made to fit some of the basic features of our data, and data derived from other experiments, it serves to illustrate only one possible mechanism to achieve concentration-dependent desensitization and bimodal response functions that are not predicted by a classical model for desensitization.

Our experiments with hypothalamic neurons have provided us with a valuable new tool to test and expand our model for α7 receptor activation. The nicotinic responses of these cells confirm much of what has been reported for α7-type nicotinic acetylcholine receptor in other systems and due to their minimal response rundown represent an excellent system for studying concentration–response dynamics. Arguably, the preparation of fresh neurons from the hypothalamus, a tissue rich in α-bungarotoxin binding in vivo, may also provide unique insight into the nature of the α7-type nicotinic acetylcholine receptors that are present in the brain. The involvement of hypothalamic histaminergic neurons with Alzheimer's pathology (Airaksinen et al., 1991) also makes them a suitable model for study of drugs with potential therapeutic application.

The α7-type nicotinic acetylcholine receptor of the tuberomammillary neurons were found to have responses that can be separated into desensitizing and steady-state (or only slowly desensitizing) components, depending on the specific agonist and concentration used. We see that, as predicted by our model, the rapid desensitization is most strongly driven by agonist concentration, such that when a steep concentration ramp is applied, responses achieve peak amplitude before concentration exchange can be completed. With shallower concentration ramps, the timing of peak responses are slower.

Further analysis of tuberomammillary neurons will be useful to generate curves for the real concentration dependence of peak and steady-state currents to compare to those generated by the model. This will serve to test and refine the model so that we can determine whether significant equilibrium activation can be achieved under conditions of prolonged agonist application. The observation that rebound currents can occur after the removal of agonist suggests that at least one component of rapid desensitization is also readily reversible. This would be consistent with a gradual reduction in fractional agonist occupancy following saturation of binding sites with a high concentration of 4OH-GTS-21.

5. Conclusion

Through the study of α7 receptor function and the use of α7-selective ligands to analyze nicotinic receptor-mediated modulation of signal transduction, we continue to gain a better understanding of how this special receptor subtype may function to mediate cellular functions including survival. Specifically, by illuminating the functional modalities of α7 nicotinic acetylcholine receptor, we better understand this receptor's potential role in neuromodulation and cytoprotection. These studies help us to define how α7 receptor activation may most effectively be addressed as a pharmacological target.

Acknowledgements

Studies were supported by Taiho Pharmaceuticals and by NIH grant NS32888-02. V.U. was supported by a fellowship from the Human Frontier Science Program. We thank Jim Boulter and Jon Lindstrom for the rat and human α7 nicotinic acetylcholine receptor clones, respectively, and Steve Heinemann for the other neuronal nicotinic receptor clones. We also thank Clare Stokes, Mike Francis, and Drs. Robert Oswald, Jon Lindstrom and Stephen Baker for helpful discussions. Single-channel simulation and idealization programs were kindly provided by Drs. Tony Auerbach, Feng Qin and Fred Sachs.

References

Airaksinen, M.S., Paetau, A., Paljärvi, L., Reinikainen, K., Riekkinen, P., Suomalainen, R., Panula, P., 1991. Histamine neurons in human hypothalamus: anatomy in normal and alzheimer diseased brains. Neuroscience 44, 465–481.

Akaike, A., Tamura, Y., Takeharu, Y., Shimohama, S., Kimura, J., 1994. Nicotine-induced protection of cultured cortical neurons against *N*-methyl-D-aspartate receptor-mediated glutamate cytotoxicity. Brain Res. 644, 181–187.

Albuquerque, E.X., Alkondon, M., Pereira, E.F.R., Castro, N.G., Schrattenholz, A., Barbosa, C.T.F., Bonfante-Cabarcas, R., Aracava, Y., Eisenberg, H.M., Maelicke, A., 1997. Properties of neuronal nicotinic acetylcholine receptors: pharmacological characterization and modulation of synaptic function. J. Pharmacol. Exp. Ther. 280, 1117–1136.

Alkondon, M., Albuquerque, E.X., 1993. Diversity of nicotinic acetylcholine receptors in rat hippocampal neurons: I. Pharmacological and functional evidence for distinct structural subtypes. J. Pharmacol. Exp. Ther. 265, 1455–1473.

Alkondon, M., Pereira, E.F.R., Wonnacott, S., Albuquerque, E.X., 1992. Blockade of nicotinic currents in hippocampal neurons defines methyllycaconitine as a potent and specific receptor antagonist. Mol. Pharmacol. 41, 802–808.

Alkondon, M., Reinhardt, S., Lobron, C., Hermsen, B., Maelicke, A., Albuquerque, E.X., 1994. Diversity of nicotinic acetylcholine receptors in rat hippocampal neurons: II. The rundown and inward rectification of agonist-elicited whole cell currents and identification of receptor subunits by in situ hybridization. J. Pharmacol. Exp. Ther. 271, 494–506.

Arendash, G.W., Sengstock, G.J., Sanberg, P.R., Kem, W.R., 1995. Improved learning and memory in aged rats with chronic administration of the nicotinic receptor agonist GTS-21. Brain Res. 674, 252–259.

Barrantes, G.E., Rogers, A.T., Lindstrom, J., Wonnacott, S., 1995. alpha-Bungarotoxin binding sites in rat hippocampal and cortical cultures: initial characterisation, colocalization with alpha7 subunits

and up-regulation by chronic nicotine treatment. Brain Res. 672, 228–236.

Boulter, J., Connolly, J., Deneris, E., Goldman, D., Heinemann, S., Patrick, J., 1987. Functional expression of two neural nicotinic acetylcholine receptors from cDNA clones identifies a gene family. Proc. Natl. Acad. Sci. U. S. A. 84, 7763–7767.

Briggs, C.A., Anderson, D.J., Brioni, J.D., Buccafusco, J.J., Buckley, M.J., Campbell, J.E., Decker, M.W., Donnelly-Roberts, D., Elliot, R.L., Gopalakrishnan, M., Holladay, M.W., Hui, Y., Jackson, W., Kim, D.J.B., Marsh, K.C., O'Neill, A.O., Pendergast, M.A., Ryther, K.B., Sullivan, J.P., Arneric, S.P., 1997. Functional characterization of the novel nicotinic receptor ligand GTS-21 in vitro and in vivo. Pharm. Biochem. Behav. 57, 231–241.

Clarke, P.B.S., Schwartz, R.D., Paul, S.M., Pert, C.B., Pert, A., 1985. Nicotinic binding in rat brain: autoradiographic comparison of [^{3}H] acetylcholine [$_3$H] nicotine and [^{125}I]-alpha-bungarotoxin. J. Neurosci. 5, 1307–1315.

Connolly, J., Boulter, J., Heinemann, S.F., 1992. α4-2β2 and other nicotinic acetylcholine receptor subtypes as targets of psychoactive and addictive drugs. Br. J. Pharmacol. 105, 657–666.

De Fiebre, C.M., Meyer, E.M., Zoltewicz, J., Henry, J.C., Muraskin, S., Kem, W.R., Papke, R.L., 1995. Characterization of a family of anabaseine-derived compounds reveals that the 3-(4)-dimethylaminocinnamylidine derivative (DMAC) is a selective agonist at neuronal nicotinic α7/[^{125}I]α-bungarotoxin receptor subtypes. Mol. Pharmacol. 47, 164–171.

Dudel, J., Franke, C.H., Hatt, H., 1990. Rapid activation, desensitization, and resensitization of synaptic channels of crayfish muscle after glutamate pulses. Biophys. J. 57, 533–545.

Frazier, C.J., Buhler, A.V., Weiner, J.L., Dunwiddie, T.V., 1998. Synaptic potentials mediated via a-bungarotoxin-sensitive nicotinic acetylcholine receptors in rat hippocampal interneurons. J. Neurosci. 18, 8228–8235.

Frisch, C., Hasenöhrl, R.U., Haas, H.L., Weiler, H.T., Steinbusch, H.W.M., Huston, J.P., 1998. Facilitation of learning after lesions of the tuberomammillary nucleus region in adult and aged rats. Exp. Brain Res. 118, 447–456.

Gopalakrishnan, M., Buisson, B., Touma, E., Giordano, T., Campbell, J.E., Hu, I., Donnelly-Roberts, D., Arneric, S.P., Bertrand, D., Sullivan, J.P., 1995. Stable expression and pharmacological properties of the human α7 nicotinic acetylcholine receptor. Eur. J. Pharm. 290, 237–246.

Gray, R., Rajan, A.S., Radcliffe, K.A., Yakehiro, M., Dani, J.A., 1996. Hippocampal synaptic transmission enhanced by low concentrations of nicotine. Nature 383, 713–716.

Hunter, B.E., De Fiebre, C.M., Papke, R.L., Kem, W.R., Meyer, E.M., 1994. A novel nicotinic agonist facilitates induction of long-term potentiation in the rat hippocampus. Neurosci. Lett. 168, 130–134.

Kabakov, A.Y., Papke, R.L., 1998. Ultra fast solution applications for prolonged gap-free recordings: controlling a Burleigh piezo-electric positioner with Clampex7. Axobits, 6–9, January.

Katz, B., Thesleff, S., 1957. A study of the ''desensitization'' produced by acetylcholine at the motor end-plate. J. Physiol. 138, 63–80.

Kihara, T., Shimohama, S., Sawada, H., Kimura, J., Kume, T., Kochiyama, H., Maeda, T., Akaike, A., 1997. Nicotinic receptor stimulation protects neurons against β-amyloid toxicity. Ann. Neurol. 42, 159–163.

Kitagawa, H., Takenouchi, T., Wesnes, K., Kramer, W., Clody, D.E., 1998. Phase I studies of GTS-21 to assess the safety, tolerability, PK, and effects on measures of cognitive function in normal volunteers. 6th International Conference on Alzheimer's Disease, abstract 765.

Klapdor, K., Hasenehrl, R.U., Huston, J.P., 1994. Facilitation of learning in adult and aged rats following bilateral lesion of the tuberomammillary nucleus region. Behav. Brain Res. 61, 113–116.

Koike, T., Martin, D.P., Johnson, J.E.M., 1989. Role of Ca^{2+} channels in the ability of membrane depolarization to prevent neuronal death induced by trophic-factor deprivation: evidence that levels of internal Ca^{2+} determine nerve growth factor dependence of sympathetic ganglion cells. Proc. Natl. Acad. Sci. U. S. A. 86, 6421–6425.

Li, Y., Papke, R.L., He, Y.-J., Millard, B., Meyer, E.M., 1999. Characterization of the neuroprotective and toxic effects of a7 nicotinic receptor activation in PC12 cells. Brain Res. 81, 218–225.

Luetje, C.W., Patrick, J., 1991. Both α- and β-subunits contribute to the agonist sensitivity of neuronal nicotinic acetylcholine receptors. J. Neurosci. 11, 837–845.

Luetje, C.W., Wada, K., Rogers, S., Abramson, S.N., Heinemann, S., Patrick, J., 1990. Neurotoxins distinguish between different neuronal nicotinic acetylcholine receptors. J. Neurochem. 55, 632–640.

Mandelzys, A., De Koninck, P., Cooper, E., 1995. Agonist and toxin sensitivities of ACh-evoked currents on neurons expressing multiple ACh receptor subunits. J. Neurophysiol. 74, 1212–1221.

Marks, M.J., Grady, S.R., Yang, J.-M., Lippiello, P.M., Collons, A.C., 1994. Desensitization of nicotine stimulated RB+ efflux from mouse brain synaptosomes. J. Neurochem. 63, 2125–2135.

Martin, E.J., Panikar, K.S., King, M.A., Deyrup, M., Hunter, B., Wang, G., Meyer, E., 1994. Cytoprotective actions of 2,4-dimethoxybenzylidene anabaseine in differentiated PC12 cells and septal cholinergic cells. Drug Dev. Res. 31, 134–141.

McGehee, D.S., Heath, M.J.S., Gelber, S., Devay, P., Role, L.W., 1995. Nicotine enhancement of fast excitatory synaptic transmission in CNS by presynaptic receptors. Science 269, 1692–1696.

Messi, M.L., Renganathan, M., Grigorenko, E., Delbono, O., 1997. Activation of α7 nicotinic acetylcholine receptor promotes survival of spinal cord motoneurons. FEBS Lett. 411, 32–38.

Meyer, E., De Fiebre, C.M., Hunter, B., Simpkins, C.E., Frauworth, N., DeFiebre, N.C., 1994. Effects of anabaseine-related analogs on rat brain nicotinic receptor binding and on avoidance behaviors. Drug Dev. Res. 31, 127–134.

Meyer, E., Kuryatov, A., Gerzanich, V., Lindstrom, J., Papke, R.L., 1998a. Analysis of 40H-GTS-21 selectivity and activity at human and rat α7 nicotinic receptors. J. Pharmacol. Exp. Ther. 287, 918–925.

Meyer, E.M., King, M.A., Meyers, C., 1998b. Neuroprotective effects of 2,4-dimethoxybenzylidene anabaseine (DMXB) and tetrahydroaminoacridine (THA) in neocortices of nucleus basalis lesioned rats. Brain Res. 786, 252–254.

Meyer, E.M., Tay, E.T., Papke, R.L., Meyers, C., Huang, G., De Fiebre, C.M., 1997. Effects of 3-[2,4-dimethoxybenzylidene]anabaseine (DMXB) on rat nicotinic receptors and memory-related behaviors. Brain Res. 768, 49–56.

Meyer, E.M., Tay, E.T., Zoltewicz, J.A., Papke, R.L., Meyers, C., King, M., De Fiebre, C.M., 1998c. Neuroprotective and memory-related actions of novel α7 nicotinic agents with different mixed agonist/antagonist properties. J. Pharmacol. Exp. Ther. 284, 1026–1032.

Nakamura, S., Takemura, M., Ohnishi, K., Suenaga, T., Nishimura, M., Akiguchi, I., Kimura, J., Kimura, T., 1993. Loss of large neurons and occurrence of neurofibrillary tangles in the tuberomammillary nucleus of patients with Alzheimer's disease. Neurosci. Lett. 151, 196–199.

Newhouse, P.A., Sunderland, T., Tariot, P.N., Blumhardt, C.L., Weingartner, H., Mellow, A., Murphey, D.L., 1988. Intravenous nicotine in Alzheimer's disease: a pilot study. Psychopharmacology 95, 171–175.

Papke, R.L., Bencherif, M., Lippiello, P., 1996. An evaluation of neuronal nicotinic acetylcholine receptor activation by quaternary nitrogen compounds indicates that choline is selective for the a7 subtype. Neurosci. Lett. 213, 201–204.

Papke, R.L., Heinemann, S.F., 1991. The role of the β4 subunit in determining the kinetic properties of rat neuronal nicotinic acetylcholine α3-receptor. J. Physiol. (London) 440, 95–112.

Papke, R.L., Millhauser, G., Lieberman, Z., Oswald, R.E., 1988. Relationships of agonist properties to the single channel kinetics of nicotinic acetylcholine receptors. Biophys. J. 53, 1–10.

Papke, R.L., Podleski, T.R., Oswald, R.E., 1986. Effects of pineal factors on the action potentials of sympathetic neurons. Cell. Mol. Neurobiol. 6, 381–396.

Papke, R.L., Thinschmidt, J.S., 1998. The correction of alpha7 nicotinic acetylcholine receptor concentration–response relationships in *Xenopus* oocytes. Neurosci. Lett. 256, 163–166.

Papke, R.L., Thinschmidt, J.S., Moulton, B.A., Meyer, E.M., Poirier, A., 1997. Activation and inhibition of rat neuronal nicotinic receptors by ABT-418. Br. J. Pharmacol. 120, 429–438.

Premkumar, L.S., Auerbach, A., 1997. Stoichiometry of recombinant *N*-methyl-D-aspartate receptor channels inferred from single-channel current patterns. J. Gen. Physiol. 110, 485–502.

Qin, F., Auerbach, A., Sachs, F., 1996. Estimating single-channel kinetic parameters from idealized patch-clamp data containing missed events. Biophys. J. 70, 264–280.

Qin, F., Auerbach, A., Sachs, F., 1997. Maximum likelihood estimation of aggregated Markov processes. Proc. R. Soc. London, Sect. B: Biol. Sci. 264, 375–383.

Saper, C.B., German, D.C., 1987. Hypothalamic pathology in Alzheimer's disease. Neurosci. Lett. 74, 364–370.

Schwartz, J.C., Arrang, J.M., Garbarg, M., Pollard, H., Ruat, M., 1991. Histaminergic transmission in mammalian brain. Physiol. Rev. 71, 1–51.

Seguela, P., Wadiche, J., Dinely-Miller, K., Dani, J.A., Patrick, J.W., 1993. Molecular cloning, functional properties and distribution of rat brain alpha 7: a nicotinic cation channel highly permeable to calcium. J. Neurosci. 13 (2), 596–604.

Shafron, D.R., Simpkins, C.E., Jebelli, B., Day, A.L., Meyer, E.M., 1997. Reduced MK801 binding in neocortical neurons after AAV-mediated transfections with NMDA R1 antisense cDNA. Brain Res., in press.

Shimohama, S., Greenwald, D.L., Shafron, D.H., Akaike, A., Maeda, T., Kaneko, S., Kimura, J., Simpkins, C.E., Day, A.L., Meyer, E.M., 1998. Nicotinic α7 receptors protect against glutamate neurotoxicity and neuronal ischemic damage. Brain Res. 779, 359–363.

Sine, S., Taylor, P., 1980. The relationship between agonist occupation and the permeability response of the cholinergic receptor revealed by bound cobra alpha-toxin. J. Biol. Chem. 255, 10144–10156.

Sine, S.M., Steinbach, J.H., 1986. Activation of acetylcholine receptors on clonal mammalian BC3H-1 cells by high concentrations of agonist. J. Physiol. 370, 357–379.

Sjak-Shie, N.N.a.M.E.M., 1993. Effects of chronic nicotine and pilocarpine administration on neocortical neuronal density and GABA uptake in nucleus basalis lesioned rats. Brain Res. 624, 181–187.

Stevens, K.E., Kem, W.R., Mahnir, V.M., Freedman, R., 1998. Selective alpha7 nicotinic agonists normalize inhibition of auditory response in DBA mice. Psychopharmacology 136, 320–327.

Uteshev, V.V., Stevens, D.R., Haas, H.L., 1996. alpha-Bungarotoxin-sensitive nicotinic responses in rat tuberomammillary neurons. Eur. J. Physiol. 432, 607–613.

Wada, H., Inagaki, N., Yamatodani, A., Watanabe, T., 1991. Is the histaminergic neuron system a regulatory center of whole-brain activity. Trends Neurosci. 14, 415–418.

Watanabe, T., Taguchi, Y., Shiosaka, S., Tanaka, J., Kubota, H., Terano, Y., Tohyama, M., Wada, H., 1984. Distribution of the histaminergic neuron system in the central nervous system of rats: a fluorescent immunohistochemical analysis with histidine decarboxylase as a marker. Brain Res. 295, 13–25.

Weiler, H.-T., Hasenöhrl, R.U., van Landeghem, A.A.L., van Landeghem, M., Brankack, J., Huston, J.P., Haas, H.L., 1998. Differential modulation of hippocampal signal transfer by tuberomammillary nucleus stimulation in freely moving rats dependent on behavioral state. Synapse 28, 294–301.

Woodruff-Pak, D.S., Li, Y., Kem, W.R., 1994. A nicotinic agonist (GTS-21), eyeblink classical conditioning, and nicotinic receptor binding in rabbit brain. Brain Res. 645, 309–317.

Zhang, Z., Coggan, J.S., Berg, D.K., 1996. Synaptic currents generated by neuronal acetylcholine receptors sensitive to alpha-bungarotoxin. Neuron 17, 1231–1240.

Zhang, Z., Vijayaraghavan, S., Berg, D.K., 1994. Neuronal acetylcholine receptors that bind α-bungarotoxin with high affinity function as ligand gated ion channels. Neuron 12, 167–177.